

# Development of Forming Limit Diagrams of Aluminum and Magnesium Sheet Alloys at Elevated Temperatures

Emilie Hsu, John E. Carsley, and Ravi Verma

(Submitted November 13, 2007)

Magnesium components are increasingly being considered for use in vehicle structures due to the potential for weight reduction, fuel economy improvement, and emission reduction. Apart from castings, magnesium sheet components can open an entirely new opportunity for mass reduction. Magnesium's poor ductility at room temperature, however, requires sheet forming to be carried out at elevated temperatures. The forming limits of magnesium alloy AZ31B-O were measured with both in-plane (Marciniak) and out-of-plane (limiting dome height) test methods at 300 °C. Forming limits of aluminum alloys 5182-O and 5754-O were also measured at room temperature and compared with published forming limit diagram data to validate the test procedures. Differences between the in-plane and out-of-plane test methods are discussed along with a description of failure modes and experimental challenges in obtaining strain localization and fracture in the appropriate locations. The plane strain forming limit (FLD<sub>0</sub>) of AZ31B at 300 °C was on the order of 67% strain, which agrees well with published data.

**Keywords** aluminum, automotive, forming limit diagram, magnesium

## 1. Introduction

Increasing use of magnesium in automotive components (Ref 1-3) can provide significant reduction of overall vehicle mass, which is a key enabler for improving fuel economy (Ref 4). Production of automotive components with wrought magnesium alloys is challenged by limited room-temperature ductility that has driven the development of elevated temperature solutions to improve formability (Ref 5-11). Although basal slip and twinning of the hexagonal close packed crystal structure are the only active deformation mechanisms at room temperature (Ref 12), more slip systems become active and other mechanisms such as diffusion, grain boundary sliding, and dislocation climb may become relevant at elevated temperatures. It is generally understood that Mg sheet can be made into useful shapes in the temperature range 230–400 °C (Ref 3). Investigations of warm stretching (Ref 1, 4, 5), warm drawing (Ref 6), and bending (Ref 11) could lead to the production of closure panels and other structural components of sheet magnesium.

This article was presented at Materials Science & Technology 2007, Automotive and Ground Vehicles symposium held September 16-20, 2007, in Detroit, MI.

Emilie Hsu, Kamax L.P., 500 West Long Lake Road, Troy, MI 48098; John E. Carsley and Ravi Verma, General Motors Research and Development Center, MC: 480-106-212, 30500 Mound Road, Warren, MI 48090; and Emilie Hsu, Department of Metals and Materials Engineering, McGill University, Montreal, Canada. Contact e-mail: john.carsley@gm.com.

The forming limit diagram (FLD), first developed by Keeler and Backhofen (Ref 13), is a useful tool for evaluating and predicting sheet metal formability. Finite element analysis (FEA) to simulate the formability of automotive panels often relies on accurate FLD models to predict and avoid failure of sheet metal for a stamping procedure. The FLD is a representation of planar strain space for proportional loading combinations of major and minor strains ranging from drawing conditions on the left, plane strain loading in the center, and biaxial stretching on the right, as depicted in Fig. 1. The forming limit curve (FLC) represents the boundary between uniform (safe) deformation and the onset of plastic instability or diffuse necking that leads to failure. The most common method for measuring sheet forming limits is the limiting dome height (LDH) test which uses a hemispherical punch (Ref 14) and circle grid analysis (CGA) to measure strains (Ref 15). Figure 2(a) is a schematic representation of the LDH test, in which a sheet blank is clamped at the binder between the upper die and the lower blank holder, while a hemispherical center punch stretches the material until failure. The ASM Handbook (Ref 16) provides a good summary of sheet metal forming including the development of FLDs, CGA, the LDH test as well as the Marciniak test (Ref 17).

While the LDH test is complicated by strain gradients due to friction, normal loading, and bending, the Marciniak test provides in-plane stretching without the influence of friction. Figure 2(b) is a schematic of the Marciniak test in which a sheet sample is mated with a carrier blank (washer) and clamped at the binder. The flat-topped punch stretches the material until failure, which should occur in the unsupported center (pole region) of the sample. Ghosh and Hecker (Ref 18) explained the differences between in-plane and out-of-plane stretching and concluded that while the LDH measurements related very well to the stamping of automotive parts, the measured out-of-plane (LDH) forming limits were larger than those of in-plane stretching. They attributed these higher limits to a different instability condition and a slower strain

localization process for out-of-plane stretching. The effects of friction, bending, and tooling geometry in the LDH test influence the migration of the fracture location from the balanced biaxial pole position toward the plane strain condition at the upper die entry radius. Strain localization and fracture in the LDH test normally occur near the line separating the punch contact and the unsupported regions of the sample.

Without the influences of bending, normal pressure and a friction condition that is difficult to quantify, the in-plane method may be more sensitive to material defects, and could provide more accurate and repeatable results that are useful for FEA simulations. NIST (Ref 19) has developed a modified Marciniak test method with a recessed punch surface in order to provide more accurate data for FEA. This development drew inspiration from Raghavan (Ref 20) who developed a Marciniak test method to generate the complete FLD using modified sample and washer (carrier blank) geometries covering linear strain paths that range from  $\epsilon_1 = -\epsilon_2$  (deep drawing) to  $\epsilon_1 = \epsilon_2$  (balanced biaxial stretching). Raghavan varied the width and notch radius of the samples as well as the hole diameter of the carrier blanks to ensure that strain localization and failure occurred within the in-plane straining region of each sample.

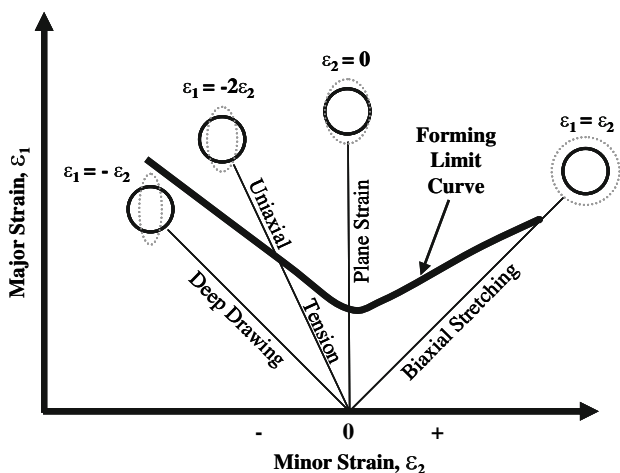


Fig. 1 Forming limit diagram

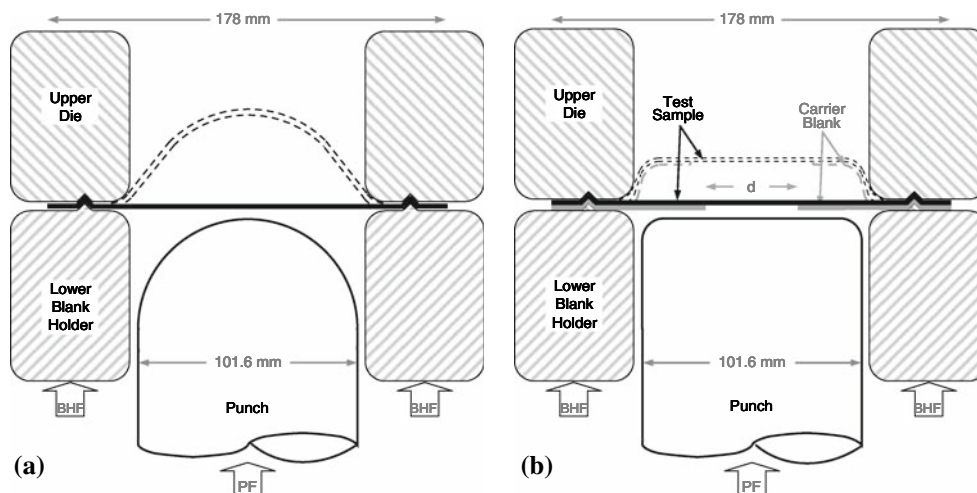


Fig. 2 Schematic of the (a) Limiting Dome Height and (b) Marciniak test setups

To investigate formability limits of Mg sheet at elevated temperatures, FLD data were generated using both the LDH and Marciniak tests with a sheet metal testing system. In development of the test procedures, two non-age-hardenable aluminum alloys (5182-O and 5754-O) were used for measuring forming limits at room temperature that were then compared to the FLC provided by an external testing service (Ref 21), as well as FLCs from General Motors' material database (Ref 22) and those provided by the material supplier (Ref 23). These aluminum alloys were also tested at 300 °C along with the AZ31B material.

## 2. Materials and Experimental Procedure

### 2.1 Materials and Sample Preparation

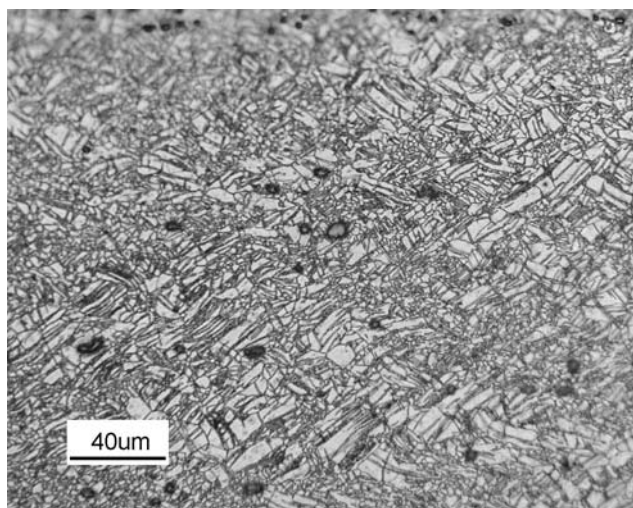
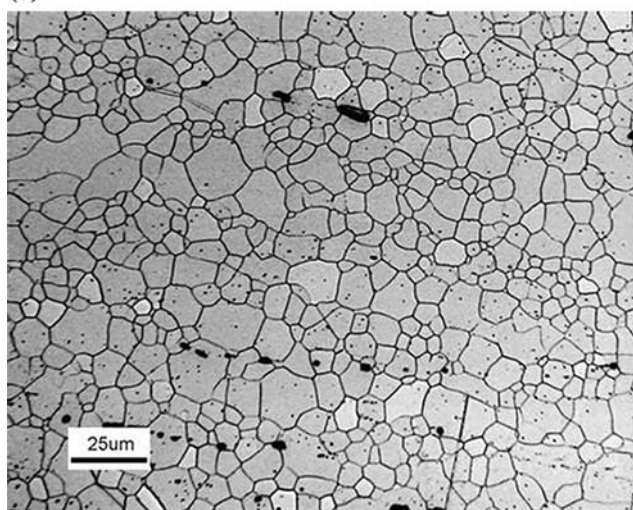
Three commercial sheet alloys, AZ31B-O (1.3 mm), AA5182-O (1.15 mm), and AA5754-O (1.0 mm), were used to develop the test methods for generating FLDs with a sheet metal testing system. The chemical compositions of these materials are shown in Table 1. Figure 3(a) shows a micrograph of the AZ31B material in the as-received condition exhibiting the heavily deformed (rolled) microstructure consisting of twins and deformation bands. The AZ31B material was annealed at 350 °C for 15 min to recrystallize the microstructure as shown in Fig. 3(b).

All sheet samples were initially sheared into either circular or square blanks of 178 mm (7 in.) diameter or edge length, respectively. Many of these blanks were further sheared or water-jet cut into various shapes in order to follow several different loading paths of the FLD. These various blank shapes were similar to those used by Raghavan (Ref 20) and are summarized in Table 2 along with the carrier blank geometries that were fabricated from all three sheet materials. All cut edges were cleaned with sandpaper to remove burrs that might prematurely initiate fracture.

The load path for balanced biaxial stretching corresponded to the 178 mm diameter circular and square blanks that were fully clamped around the periphery. Approximately plane strain loading corresponded to 76.2-101.1 mm (3-4 in.) wide samples, while 38.1 mm (1.5 in.) wide samples were used to approximate uniaxial loading.

**Table 1** Chemical compositions of AZ31B, AA5182, and AA5754

	Mg	Al	Zn	Mn	Fe	Cu	Si	Ni	Ti	Ca
AZ31B	Bal.	3.1	1.0	0.42	0.006	0.003	<0.1	<0.003	...	<0.01
AA5182	4.3	Bal.	<0.01	0.34	0.21	<0.01	0.03	<0.01	<0.01	...
AA5754	3.0	Bal.	<0.01	0.24	0.26	0.02	0.03	<0.01	<0.01	...

**(a)****(b)****Fig. 3** Microstructure of AZ31B Mg sheet: (a) as-received condition (as hot-rolled sheet) and (b) O-temper (after annealing)

All aluminum and magnesium samples were prepared for CGA by electrochemical etching with a stencil pattern of 2.54 mm diameter circles. Aluminum blanks were etched with 250A<sup>1</sup> electrolytic solution, while the magnesium samples were etched with LNC-4<sup>1</sup> and washed with Formula 3 Cleaner.<sup>1</sup>

## 2.2 Forming Procedures

A sheet metal testing system, SP150,<sup>2</sup> was used with the LDH die set for out-of-plane testing and the Marciniak die set

for in-plane testing. The SP150 is a double-action servo-hydraulic press with a fully closed-loop control system consisting of a guided lower platen actuator (clamp) rated at 68,000 kgf (75 tons) and a center actuator (punch) rated at 45,000 kgf (50 tons). The upper die and lower blank holder were heated with band heaters capable of 300 °C. The LDH and Marciniak punches contain cartridge heaters that were also capable of maintaining 300 °C. The upper and lower sections were enveloped in Cer-Wool<sup>®</sup> ceramic fiber to reduce heat loss during operation. K-type thermocouples were attached to several aluminum blanks, and temperature set points for the punch and die sections were adjusted to provide steady-state conditions at approximately 300 °C.

Both LDH and Marciniak tests were performed with AA5182-O and AA5754-O at room temperature to validate the test procedures by comparison with FLCs that were determined for these same lots of material by the Industrial Research and Development Institute (IRDI) (Ref 21). Both test methods were also performed at 300 °C with both aluminum alloys as well as with AZ31B. Square or circular sheet metal blanks were aligned with the lower blank holder surface prior to clamping. Alignment is especially important when using a carrier blank with the Marciniak tooling because the center hole of the carrier must be symmetrical with the punch in order to provide uniform straining in the pole region of the test sample. After a sample was aligned, it was clamped to a preset load, typically ranging from 18,000 to 55,000 kgf (40,000-120,000 lbs). The clamp beads prevented material draw-in during the test so that all deformation was under pure stretch conditions. Next, the punch was actuated to travel at a constant rate, engage the sample, and stretch until failure. After surpassing a minimum load threshold, the setting for which depends on test temperature, sample properties, and thickness, the program stopped when it sensed a preset load drop, typically on the order of 1-10%. For FLD determination, it is most desirable to stop the test at the onset of incipient necking in order to measure strains corresponding to the forming limit curve. However, strain localizes quickly in aluminum samples and fracture often occurs before the load drop sensitivity can halt the test. Data included punch load and displacement and clamp load and displacement as a function of time. The punch loading rate was quasi-static at 0.127 mm/s (0.005 in./s) for all tests. For room temperature testing, oil was applied to the aluminum samples. Boron nitride and graphite lubricants were used for testing at elevated temperatures.

## 2.3 Strain Measurement

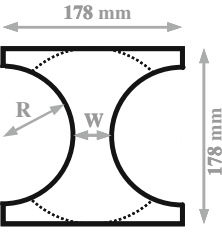
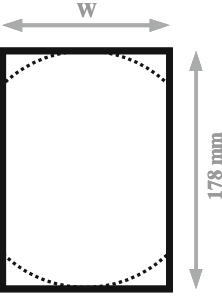
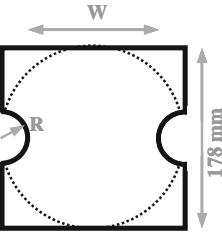
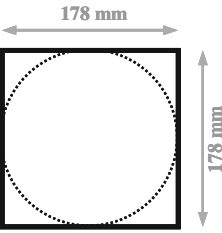
Circle grid analysis was used to measure the engineering major and minor strains of the deformed circles on the outer surface of the deformed samples. A camera<sup>3</sup> was used to capture images of the deformed circles near the fracture while the Grid Pattern Analyzer GPA 3.0 software recorded the data.

<sup>1</sup>Chemical etch electrolyte from Lectroetch<sup>®</sup>.

<sup>2</sup>Interlaken Technologies Corporation, Chaska, MN.

<sup>3</sup>ASAME technology LLC.

**Table 2 Sample and carrier blank geometries for the Marciniak and LDH test methods**

	Sample type	Effective width, $W$ , mm	Notch radius, $R$ , mm	Carrier blank hole diameter, $d$ , mm
	Type I	38.1	69.9 76.2	n/a
	Type II	76.2 101.1 120.7 127.0	n/a	22.9 38.1 40.6
	Type III	76.2 127.0	25.4	22.9 38.1 40.6
	Type IV	178	n/a	22.9 30.5 35.6 38.1 40.6

Data was plotted on a forming limit diagram as represented in Fig. 1 and the forming limit curves were estimated as the boundary between the uniformly strained area and localized strain or fractured areas.

### 3. Results and Discussion

#### 3.1 Aluminum Alloys at Room Temperature

The Marciniak test method was used to stretch samples to determine the forming limit diagrams for both aluminum alloys. Figure 4 shows three AA5182 samples of different widths, and thus strain paths, from which deformed circles were measured to determine necking strains. In each case, the crack formed in the unsupported region of the sample, near the pole and propagated perpendicular to the rolling direction. The FLD for

1.15 mm thick AA5182-O at room temperature is shown in Fig. 5 with a plane strain limit  $FLD_o$  of  $\sim 18\%$ . The forming limit curve was drawn above the good data points to define the lower bound of the necking zone. A second curve was included to describe the boundary between the necking and fracture zones. For comparison, the FLC determined for this same lot of material by an external source (Ref 21) is also shown, which agrees well with the current measurements.

Further comparison is provided by the FLCs from GM's material database (Ref 22) and the material supplier (Ref 23). These FLCs suggest that AA5182 would have slightly greater formability ( $FLD_o$  approximately 22-23%) than determined here. This observation is consistent with Ghosh and Hecker (Ref 18) because these values of the FLC were determined by the out-of-plane, LDH test method which supposedly estimates higher forming limits than the in-plane, Marciniak test method.

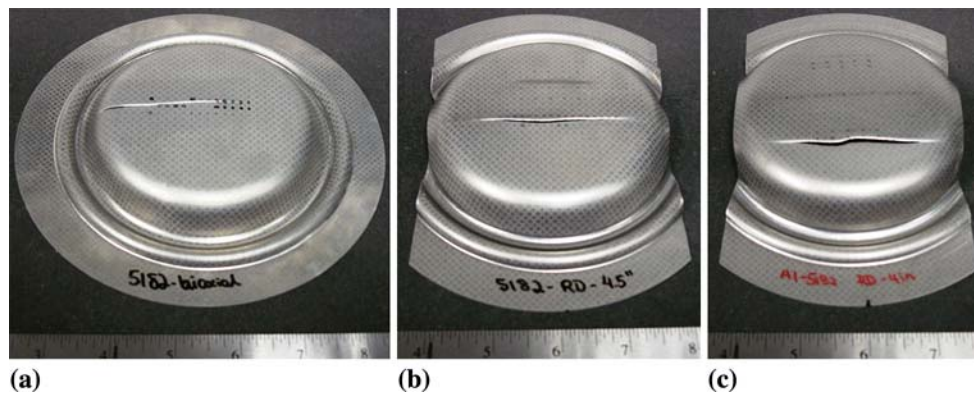


**Fig. 4** AA5182-O samples stretched to failure with the Marciniak die set at room temperature. (a) Balanced biaxial strain path (178 mm dia), (b) near plane strain path (114 mm width), and (c) near plane strain path (101.6 mm width)

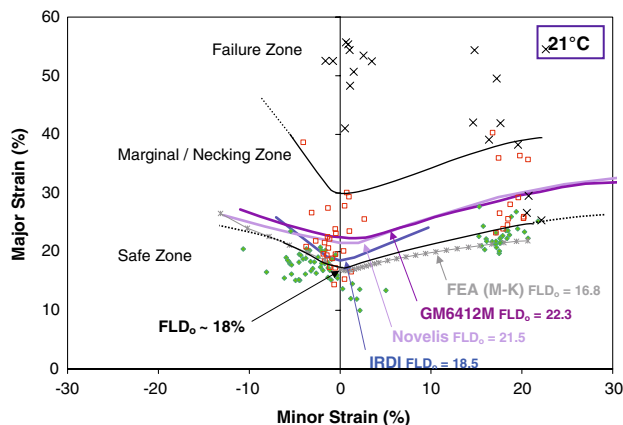


**Fig. 5** Forming Limit Diagram for AA5182-O, 1.15 mm, at room temperature. The blue curve represents the FLC for this material determined by IRDI (Ref 21) in which the Marciniak test method was used. The dark and light purple curves represent the FLCs from GM's material database (Ref 22) and from Novelis (Ref 23), respectively, in which the LDH method was used. The gray curve is the FEA-calculated FLC for this alloy (Ref 24) using the M-K method

Yet another comparison is provided by the FLC in Fig. 5 that was calculated for this material using finite element analysis based on the Marciniak-Kuczinski method with Barlat's anisotropic material model, YLD2000-2D, and the Voce hardening law (Ref 24). It has been suggested that the Voce hardening law provides a more accurate estimation of sheet metal forming limits for anisotropic aluminum alloys than does the power law (Ref 25). The FLC strain values taken from Abedrabbo et al. (Ref 24) were converted from true strain to engineering strain for comparison in Figs. 5, 6, and 9 by the simple relationship  $\epsilon = \ln(1 + e)$ , which is a valid assumption in the uniform deformation regime. The calculated FLC agrees very well with the experimental data in Fig. 5, although it might appear to be slightly conservative, especially on the right side of the FLD. This is expected since FEA-determined FLCs represent the onset of localization, which is very difficult to determine experimentally. For more information on the calculation of coefficients for Barlat's models as a function of temperature, see Abedrabbo et al. (Ref 26, 27).

Figure 6 shows the FLD for 1.0 mm AA5754-O at room temperature. Although fewer data points were measured for this

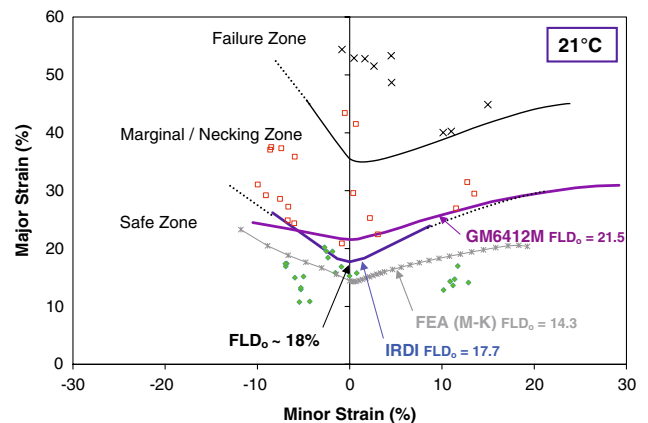


**Fig. 6** Forming Limit Diagram for AA5754-O, 1.00 mm, at room temperature using the Marciniak test method. The blue curve represents the FLC for this material produced by IRDI (Ref 21), while the gray curve is the FEA-calculated FLC (Ref 24). For comparison, the LDH-determined FLC from GM's material database is also included (Ref 22)

alloy, the curve from IRDI (Ref 21) agrees very well with the current analysis. However, the FEA-determined FLC for this material (Ref 24) is considerably lower than the measured data.

### 3.2 Marciniak Test Method at Room Temperature

The use of a carrier blank in the Marciniak test method was intended to provide uniform straining in the pole region of the sample without contact friction with the punch, and to promote strain localization and fracture in this unsupported region. However, localization and fracture often did not occur near the pole of the sample. Premature fracture often occurred at the upper die entry radius that was in direct contact with the upper surface of the sample as indicated in Fig. 7(a) and 8(b). This failure mode was most prevalent with samples that were sheared to widths of 101.1-127 mm (4-5 in.), and could be somewhat alleviated by slightly reducing the blank holder force, but still preventing material draw-in during the test. This may have been due to shear localization at the binder. Preparing the blanks with a notch radius as described in Table 2 helped to delay failure at the die entry by orienting the trimmed edge at a

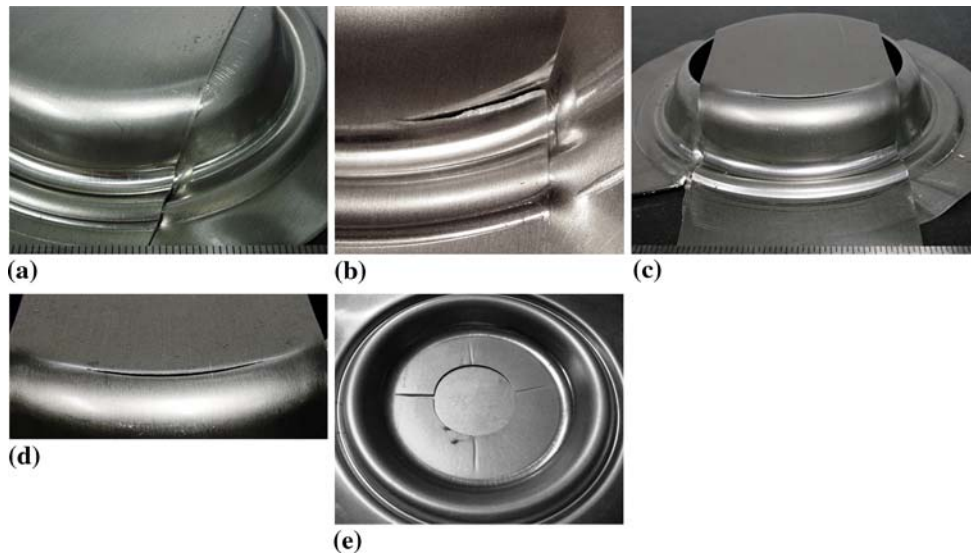


**Fig. 7** Room temperature failure modes for Marciniak samples. (a) plane strain 5754 sample with failure at the upper die entry radius, (b) magnified image of the entry radius failure in (a), (c) plane strain 5182 sample with failure initiated along the line of contact with hole edge of the carrier blank, (d) magnified image the edge contact failure in (c), (e) biaxial 5182 sample showing failure in the carrier blank initiating from the expanding edge of the center hole

right angle to the circular binder of the tool, which also should have reduced the stress concentration to enable more uniform strain distribution.

Figure 7(c) and (d) also shows that some samples cracked along the edge of the hole of the carrier blank. Obviously such samples were not useful for measuring necking or failure strains with CGA, and these premature failures made it difficult to fill in the left side of the FLD. This failure mode may have been avoided by optimizing the hole diameter of the carrier blank, which could be done with finite element analysis.

Another example of premature “failure” is when the carrier blank developed radial cracks emanating from the center hole (Fig. 7e). More experimentation is needed to optimize the hole diameter and lubrication as a function of sheet thickness and inherent material formability.

### 3.3 Marciniak Test Method at 300 °C

Testing materials at elevated temperature required the use of high-temperature lubricants such as boron nitride (BN) and graphite. These lubricants were applied to one or both sides of the carrier blank, but the best results were obtained when lubricant was only applied to the surface that was in contact with the punch. In addition to the room-temperature failure modes shown in Fig. 7, samples also failed by other modes at 300 °C. Figure 8(a) illustrates strain localization and crack initiation in the ‘plane-strain’ portion of the cup wall, along the upper die entry radius. Cracking also occurred at or just below the punch radius as shown in Fig. 8(b) and (c), respectively. Strain localization or necking just below the punch radius is very reminiscent of similar behavior observed during Superplastic or Quick Plastic Forming (Ref 28-31) in which a sheet metal is blow-formed into a female die cavity over a die entry radius. As the sheet slides over the radius, necking often occurs due to localized compressive stress (Ref 29, 31). The solution for that situation was to remove the lubricant and enhance static friction as the sheet contacted the die surface. In that case, the sheet was unable to slide across the tool and hence necking was

avoided. In the Marciniak test method, however, it is desirable for the carrier blank to slide over the punch radius in order to promote uniform straining near the pole of the sample. Graphite is far more lubricious than BN at 300 °C and did enable significantly greater depths of stretching, but the failure mode remained unchanged.

No combination of lubricant, carrier blank geometry, or hole size provided a technique to induce strain localization and cracking in the unsupported pole region for either aluminum alloy or for AZ31B. All 300 °C Marciniak test samples failed by one of the modes illustrated in Fig. 8. Without strain localization or cracking near the pole of these test samples, the forming limits could not be estimated by this method. Figure 9 shows the forming strains in the pole region of 1.0 mm AA5754-O samples tested with the Marciniak method at 300 °C. Since there were no strain localizations or cracking in these pole regions, the forming limits could not be determined, but reasonably lie somewhere above the black dotted line in Fig. 9 ( $FLD_0$  should be greater than 28%). For comparison, the room temperature FLD from IRDI is included, which illustrates that forming-wrought aluminum at elevated temperature does provide significantly greater formability. Also included in Fig. 9 are FLCs calculated with FEA for this alloy at increasing temperatures (Ref 24). The FLC for the highest temperature estimated by FEA (260 °C) suggests quite an increase in the plane strain forming limit. Based on the trend implied by the calculations,  $FLD_0$  for AA5754-O at 300 °C should be significantly greater than 36%. It may be advantageous to test this material with the LDH punch in order to determine the necking limits at higher temperatures.

A better solution may be realized in a re-design of the Marciniak test method. The Marciniak punch radius in these tests was 10 mm. Perhaps a significantly larger radius, with corresponding decrease in the flat area could distribute strain more uniformly around the punch contact area in order to promote strain localization in the pole region rather than at the locations indicated in Fig. 8. Of course, the proper combination of carrier blank geometry with test sample shape for measuring

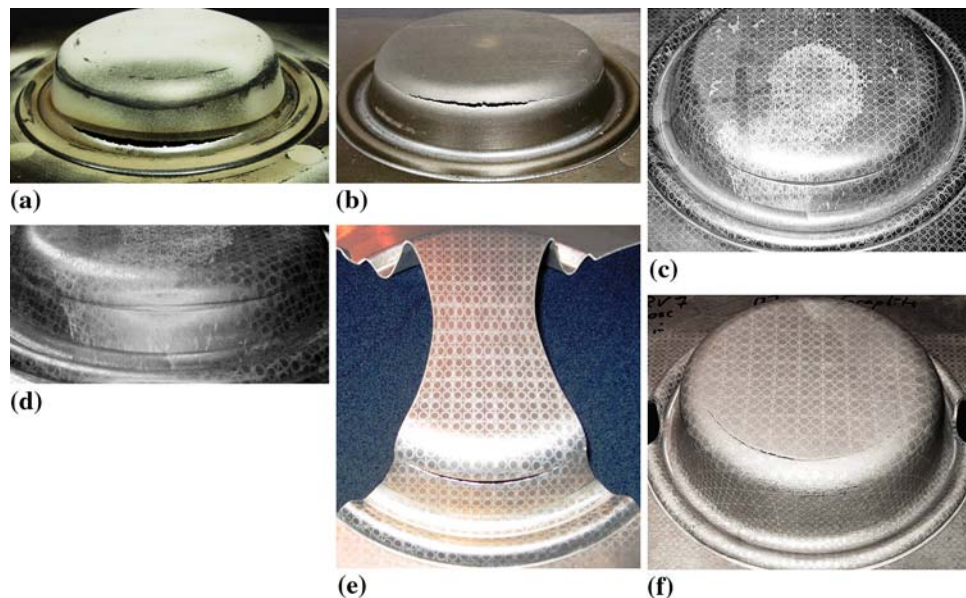


**Fig. 8** Elevated temperature failure modes for Marciniak samples. (a) biaxial AZ31B sample with BN lubricant that failed at the upper die entry radius, (b) biaxial AZ31B sample with BN lubricant that failed at the punch radius, (c) biaxial 5182 sample with failure just below the punch radius, (d) plane strain 5182 sample with localized neck formation just below the punch radius and failure at the upper die entry radius, (e) narrow 5754 sample with failure just below the punch radius, (f) plane strain AZ31B sample with graphite lubricant that failed along the line of contact with the hole edge of the carrier blank

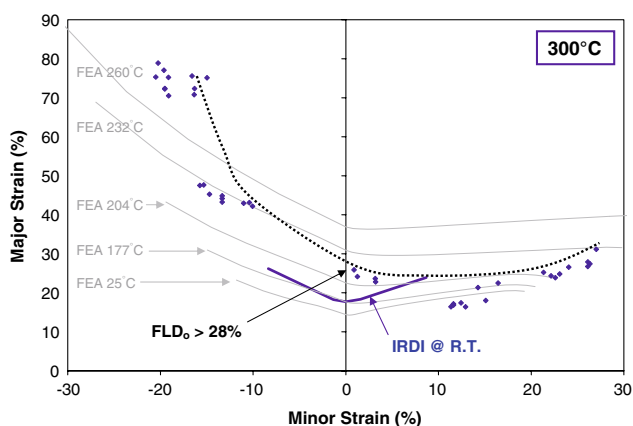


**Fig. 9** Forming Limit Diagram for AA5754-O, 1.00 mm, 300 °C using the Marciniak test method. All data points on this chart represent “good” measurements since the tests did not reveal strain localization or fracture in the unsupported, pole region of any sample. The FLC for 300 °C would lie somewhere above the dotted line, and the plane strain limit should be greater than 28%. For comparison, the blue curve represents the FLC for this material at room temperature (Ref 21). The gray curves represent the FEA-calculated FLCs for this material at the various elevated temperatures indicated (Ref 24)

forming limits along the various strain paths would require further development.

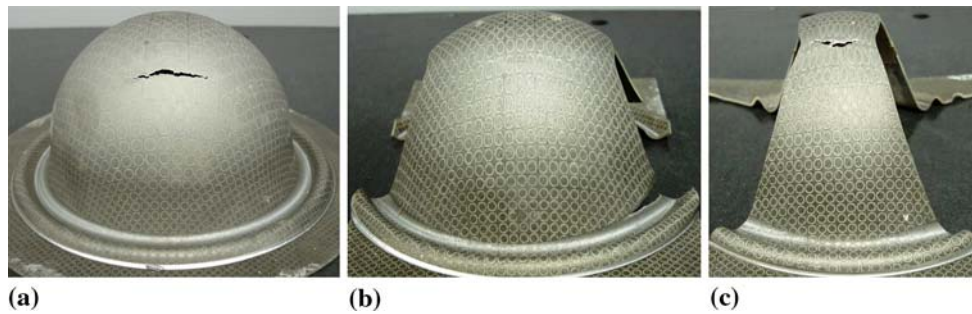
### 3.4 Forming Limit Diagram of AZ31B

Room temperature testing of 1.3 mm AZ31B was not possible with the current die sets because all samples fractured when load was applied to the clamp bead. Perhaps a different lock bead design could enable testing, but room temperature formability of magnesium sheet alloys is typically very poor.

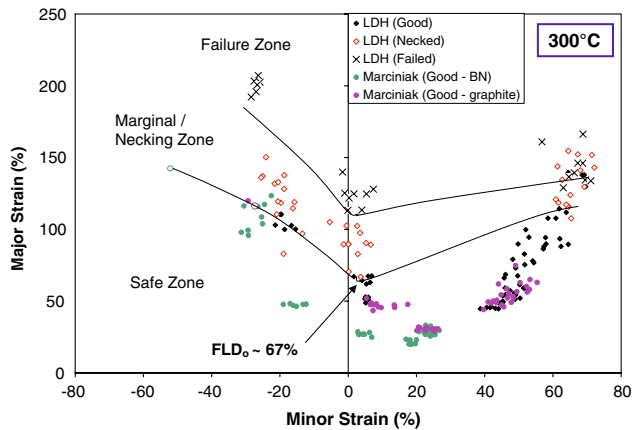
With the test environment stable at 300 °C, magnesium samples were set on the lower die and allowed to heat for 2 min prior to clamping, then for another 2 min prior to actuating the punch. All samples tested with the Marciniak punch failed by one of the modes illustrated in Fig. 8. Therefore, the LDH test method was used to determine the forming limit curve for AZ31B at 300 °C with BN lubricant applied between the sample and the punch.

Figure 10 displays AZ31B LDH samples tested at 300 °C that were subjected to several different loading paths and were useful for determining the FLC. Based on several repeated tests for each path, there did not appear to be any specific preferred fracture orientation for the biaxial stretch samples. This is unlike other AZ31B samples that were stretched in a balanced biaxial mode by bulging with air at elevated temperatures (Ref 32). In that situation, samples tended to tear at the top of the dome and along the rolling direction. Since friction is inherent in the LDH test, samples tended to fail at the line of contact between the punch and the unsupported region of the sample, away from the pole of the dome. As a result, deformed circles near the fractured region from the biaxial stretch test exhibited ellipsoidal rather than circular shapes. Although these measurements do not represent the balanced biaxial stretch zone, they were still considered good data for the FLD.

The forming limit diagram for 1.3 mm AZ31B-O determined at 300 °C using a quasi-static punch speed of 0.127 mm/s (0.005 in./s) is shown in Fig. 11. The plane strain forming limit,  $FLD_0$ , was found to be approximately 67%, which is a remarkable improvement relative to its room temperature formability. Also included in this chart are the CGA measurements of “good” data points from the Marciniak test method. All of these data points lie below the FLC because necking and failure did not occur near the pole region of the Marciniak samples. The FLC drawn from the LDH data agree somewhat with the FLC presented by Chen et al. (Ref 7), although their curve suggested a slightly higher  $FLD_0$  for AZ31B at 300 °C



**Fig. 10** Magnesium LDH samples deformed to failure under different loading paths. (a) biaxial stretching, (b) plane strain deformation, (c) drawing condition with negative minor strain



**Fig. 11** Forming limit diagram for AZ31B-O, 1.3 mm gage, at 300 °C

that is approximately 73% (0.55 true strain). Siegert and Jäger (Ref 9) also reported on the forming limits of AZ31B at 280 and 350 °C. Interpolating their data for approximately 300 °C suggests that  $FLD_o$  might be in the neighborhood of about 65% (0.5 true strain) based on plane strain tensile testing. Interpolating Siegert and Jäger's (Ref 9) data for balanced biaxial stretching and uniaxial tensile limit strains also agree well with the current results shown in Fig. 11.

Limiting dome height is often used as a measure of sheet formability. In this study, the LDH values obtained with the AZ31B magnesium sheet at 300 °C were in the range 60–65 mm. For the hemispherical punch of diameter 101.6 mm, this gives an LDH-to-diameter ratio of 0.59–0.64. This is a high level of formability by any standard. Part of the reason for this high LDH is the shift of the failure away from the pole region due to friction between the punch and the sheet despite liberal application of lubricant. This is evident from the comparison of the circle grid pattern at the pole and away from the pole regions, in Fig. 10(a). The redistribution of strain away from the potentially high-strain area helps provide the high formability. It will be interesting to compare the LDH (or LDH-to-diameter ratio) obtained in this study with one obtained with gas-pressure forming under the same test temperature and strain rate conditions, since the latter will have no frictional effects.

#### 4. Summary

Formability of magnesium sheet was greatly enhanced by deforming at elevated temperature such that the plane strain

forming limit of AZ31B was measured as 67% (0.51 true strain) at 300 °C, which is in good agreement with the literature. The forming limit diagram for AZ31B at 300 °C was developed using both in-plane (Marciniak) and out-of-plane (LDH) test methods. The LDH test is complicated by the effects of friction, bending strain, and normal pressure on the sheet samples that often lead to results suggesting higher forming limits than are typically determined via the Marciniak test method. Since the in-plane Marciniak test does not include these attributes, it has been suggested as a better tool for distinguishing materials based on inherent material behavior.

The apparent forming limit curves for aluminum alloys at room temperature were shown to be higher with the LDH test method than with the in-plane test method. This result supports existing arguments in the literature claiming that while the LDH test results may provide better correlation with actual panel stamping trials, the Marciniak test results should provide more accurate depiction of material behavior useful for comparison by finite element simulation.

The Marciniak test method requires greater care in setup with a matching carrier blank that transfers load between the punch and the test sample in order to promote strain localization in the pole region. However, when testing sheet metal at elevated temperatures with the Marciniak method, no combination of sample shape, lubrication, and carrier blank geometry was found to promote strain localization and fracture near the pole region. Hence, the FLC could not be estimated. Instead, the LDH method provided samples useful for measuring the limit strains and determining the shape of the FLC of AZ31B at 300 °C. Further development is needed to refine the Marciniak test method such that strain can localize in the pole region. This may require a re-design of the flat-top punch geometry to avoid sample fracture at undesirable locations.

#### References

1. A.A. Luo, Material Comparison and Potential Applications of Magnesium in Automobiles, *Magnesium Technology 2000*, H.I. Kaplan, J. Hryn, and B. Clow, Eds., TMS, 2000, p 89–98
2. P.E. Krajewski, "Elevated Temperature Forming of Sheet Magnesium Alloys," SAE Book Number: SP-1683, SAE Paper No. 2001-01-3104
3. B.L. Mordike and T. Ebert, Magnesium – Properties – Applications – Potential, *Mater. Sci. Eng. A*, 2001, **302**, p 37–45
4. B. Passek, Light Weight Design in Body-in-White Development Considering Passive Safety Requirements, *Proceedings of 2001 ASME International Mechanical Engineering Congress and Exposition*, November 2001 (New York, NY), AMD Vol. 251, IMECE2001/AMD-25440, 2001



5. H. Watanabe, H. Tsutsui, T. Mukai, M. Kohzu, S. Tanabe, and K. Higashi, Deformation Mechanism in a Coarse-Grained Mg-Al-Zn Alloy at Elevated Temperatures, *Int. J. Plast.*, 2001, **17**, p 387–397
6. E. Doege and K. Dröder, Sheet Metal Forming of Magnesium Wrought Alloys – Formability and Process Technology, *J. Mater. Process. Technol.*, 2001, **115**, p 14–19
7. F.-K. Chen and T.-B. Huang, Formability of Stamping Magnesium-Alloy AZ31 Sheets, *J. Mater. Process. Technol.*, 2003, **142**, p 643–647
8. K. Siegert, S. Jäger, and M. Vulcan, Pneumatic Bulging of Magnesium AZ 31 Sheet Metals at Elevated Temperatures, *CIRP Ann. –Manuf. Technol.*, 2003, **52**, p 241–244
9. K. Siegert and S. Jäger, “Warm Forming of Magnesium Sheet Metal,” SAE Technical Paper 2004-01-1043, reprinted from Sheet/Hydro/Gas Forming Technology and Modeling (SP1840)
10. D.L. Yin, K.F. Zhang, G.F. Wang, and W.B. Han, Warm Deformation Behavior of Hot-Rolled AZ31 Mg Alloy, *Mater. Sci. Eng. A*, 2005, **392**, p 320–325
11. J.E. Carsley and S. Kim, Warm Hemming of Magnesium Sheet, *J. Mater. Eng. Perform.*, 2007, **16**, p 331–338
12. H. Li, E. Hsu, J. Szpunar, R. Verma, and J.T. Carter, Determination of Active Slip/Twinning Modes in Mg Alloy Near Room Temperature, *J. Mater. Eng. Perform.*, 2006, **16**, p 321–326
13. S.P. Keeler and W.A. Backofen, Plastic Instability and Fracture in Sheets Stretched Over Rigid Punches, *ASM Trans. Quart.*, 1963, **56**, p 25–48
14. “Standard Test Method for Determining Forming Limit Curves,” ASTM E 2218-02
15. R.A. Ayres, Aids for Evaluating Sheet Metal Formability: The Limiting Dome Height (LDH) Test and the Circle Grid Analyzer, *Novel Techniques in Metal Deformation Testing*, R.H. Wagoner, Ed., TMS, 1983, p 47–64
16. B. Taylor, Sheet Formability Testing, *Metals Handbook, 9th ed., Vol. 8, Mechanical Testing*, American Society for Metals, 1985, p 547–570
17. Z. Marciniak and K. Kuczynski, Limit Strains in the Processes of Stretch-Forming Sheet Metal, *Int. J. Mech. Sci.*, 1967, **9**, p 609–620
18. A.K. Ghosh and S.S. Hecker, Stretching Limits in Sheet Metals: In-Plane Versus Out-of-Plane Deformation, *Metall. Trans.*, 1974, **5**, p 2161–2164
19. T. Foecke, S.W. Banovic, and R.J. Fields, Sheet Metal Formability Studies at the National Institute of Standards and Technology, *JOM*, 2001, **53**, p 27–30
20. K.S. Raghavan, A Simple Technique to Generate In-Plane Forming Limit Curves and Selected Applications, *Metall. Mater. Trans. A*, 1995, **26A**, p 2075–2084
21. “Determination of the Experimental FLD for 9 Aluminum Alloy Sheet Materials (Project #240 290),” Industrial Research+Development Institute, 20 December 2002
22. GM Formability Database – GM6412M – Grades AL115N1 (5182) and AL90N3 (5754), prepared by Susan Hartfield-Wunsch, 7 March 2001
23. A. Brooks, Novelis Corporation, private communication, 31 July 2007
24. N. Abedrabbo, F. Pourboghra, and J. Carsley, Forming of AA5182-O and AA5754-O at Elevated Temperatures Using Coupled Thermo-Mechanical Finite Element Models, *Int. J. Plast.*, 2007, **23**, p 841–875
25. M. Aghaie-Khafri and R. Mahmudi, Prediction of Plastic Instability and Forming Limit Diagrams, *Int. J. Mech. Sci.*, 2004, **46**, p 1289–1306
26. N. Abedrabbo, F. Pourboghra, and J. Carsley, Forming of Aluminum Alloys at Elevated Temperatures – Part 1: Material Characterization, *Int. J. Plast.*, 2006, **22**, p 314–341
27. N. Abedrabbo, F. Pourboghra, and J. Carsley, Forming of Aluminum Alloys at Elevated Temperatures – Part 2: Numerical Modeling and Experimental Verification, *Int. J. Plast.*, 2006, **22**, p 342–373
28. R. Verma, P.A. Friedman, A.K. Ghosh, C. Kim, and S. Kim, Superplastic Forming Characteristics of Fine-grained 5083 Aluminum, *J. Mater. Eng. Perform.*, 1995, **4**, p 543–550
29. R. Verma, J.T. Carter, and P.E. Krajewski, “Assessment of AZ31 Mg Sheet for Automotive Applications,” Presented at the *Light Metals Technology 2007*, Sep 24–26, 2007, Saint Sauveur, Quebec, Canada
30. N.R. Harrison, S.G. Luckey, P.A. Friedman, and Z.C. Xia, Influence of Friction and Die Geometry on Simulation of Superplastic Forming of Al-Mg Alloys, *Advances in Superplasticity and Superplastic Forming*, E.M. Taleff, P.A. Friedman, P.E. Krajewski, R.S. Mishra, and J.C. Schroth, Eds., TMS, 2004, p 301–309
31. S.G. Luckey, P.A. Friedman, and Z.C. Xia, Aspects of Element Formulation and Strain Rate Control in Numerical Modeling of Superplastic Forming, *Advances in Superplasticity and Superplastic Forming*, E.M. Taleff, P.A. Friedman, P.E. Krajewski, R.S. Mishra, and J.C. Schroth, Eds., TMS, 2004, p 371–380
32. J.T. Carter, R. Verma, and P.E. Krajewski, “Mechanical Behavior of AZ31 Sheet Materials at Room and Elevated Temperature,” to be presented at the *2008 TMS Annual Meeting in New Orleans, LA*, and to be published in “Magnesium Technology 2008”